

University of Nebraska - Lincoln

DigitalCommons@University of Nebraska - Lincoln

Anthony F. Starace Publications

Research Papers in Physics and Astronomy

March 1972

Potential-Barrier Effects in Photoabsorption. III. Application to 4d-Shell Photoabsorption in Lanthanum

J.L. Dehmer

University of Chicago, Chicago, Illinois

Anthony F. Starace

University of Nebraska-Lincoln, astarace1@unl.edu

Follow this and additional works at: <https://digitalcommons.unl.edu/physicsstarace>



Part of the [Physics Commons](#)

Dehmer, J.L. and Starace, Anthony F., "Potential-Barrier Effects in Photoabsorption. III. Application to 4d-Shell Photoabsorption in Lanthanum" (1972). *Anthony F. Starace Publications*. 17.

<https://digitalcommons.unl.edu/physicsstarace/17>

This Article is brought to you for free and open access by the Research Papers in Physics and Astronomy at DigitalCommons@University of Nebraska - Lincoln. It has been accepted for inclusion in Anthony F. Starace Publications by an authorized administrator of DigitalCommons@University of Nebraska - Lincoln.

tion on which this calculation is based, namely, that the lanthanides give up three electrons for bonding in the metal. The present interpretation of the absorption spectra provides the most detailed confirmation of this.

The lanthanides that remain to be treated and for which the data are available in Refs. 1 and 2 are Nd, Sm, and Dy. These are complex cases because of the size of the matrices needed but the methods of treatment are the same. The lanthanides show this detailed structure because the unfilled $4f$ shell is collapsed and therefore not subject to large interactions with the environment, and because of the large electrostatic interaction with the $4d$ shell.

The same set of circumstances probably exists in the actinides where the interaction is between the $5d$ and $5f$ shells. It would therefore be of interest to see the absorption experiments carried out for the actinide period.

ACKNOWLEDGMENTS

I am pleased to thank Professor Ugo Fano who brought this problem to my attention and suggested the approach which led to these results, Dr. Robert Cowan for kindly providing an independent calculation of the relative intensities in Pr utilizing the parameters given here, and Dr. John Cooper for rewarding discussions.

¹J. M. Zimkina, V. A. Fomichev, S. A. Gribovskii, and I. I. Zhukova, *Fiz. Tverd. Tela* **9**, 1447 (1967); **9**, 1490 (1967) [*Sov. Phys. Solid State* **9**, 1128, (1967); **9**, 1163 (1967)].

²R. Haensel, P. Rabe, and B. Sonntag, *Solid State Commun.* **8**, 1845 (1970).

³J. L. Dehmer, A. F. Starace, U. Fano, J. Sugar, and J. W. Cooper, *Phys. Rev. Letters* **26**, 1521 (1971).

⁴A. F. Starace, preceding paper, *Phys. Rev. B* **5**, 1773 (1972), Paper I of this series.

⁵W. H. Zachariasen, in *The Metal Plutonium*, edited by A. S. Coffinberry and W. R. Miner (University of Chicago Press, Chicago, 1961), p. 99.

⁶W. T. Carnall, P. R. Fields, and K. Rajnak, *J. Chem. Phys.* **49**, 4424 (1968); **49**, 4443 (1968); **49**, 4447 (1968); **49**, 4450 (1968).

⁷G. Racah, *Phys. Rev.* **62**, 438 (1942); **63**, 367 (1943); **76** 1352 (1949).

⁸U. Fano, F. Prats, and Z. Goldschmidt, *Phys. Rev.* **129**, 2643 (1963).

⁹A. P. Jucys, J. B. Ievinsonas, and V. V. Vanagas,

Mathematical Apparatus of the Theory of Angular Momentum, Publ. No. 3 (Akad. Nauk. Lit. SSR Inst. Fiz. Mat., Vilnius, USSR, 1960).

¹⁰C. W. Nielson and G. F. Koster, *Spectroscopic Coefficients for the p^N , d^N , and f^N Configurations* (MIT Press, Cambridge, Mass., 1963).

¹¹G. Racah, *Bull. Res. Council Israel* **8F**, 1 (1959).

¹²C. Froese, *Can. J. Phys.* **41**, 1895 (1963).

¹³J. A. Bearden, *Rev. Mod. Phys.* **39**, 78 (1967).

¹⁴J. Sugar and V. Kaufman (unpublished).

¹⁵R. D. Cowan, *J. Opt. Soc. Am.* **58**, 808 (1968).

¹⁶L. Brewer, *J. Opt. Soc. Am.* **61**, 1101 (1971).

¹⁷In Refs. 5 and 16 it is pointed out that Yb should be divalent in the metal. As such, it should show no absorption since the $4f$ shell would be full. It has been reported that absorption from the $3d$ shell in Yb occurs as one line in the oxide but not at all in the metal [F. H. Combley, E. A. Stewardson, and J. E. Wilson, *J. Phys. B* **1**, 120 (1968)]. It would therefore appear that the Yb absorption reported in Ref. 1 arose from the trivalent oxide.

Potential-Barrier Effects in Photoabsorption. III. Application to $4d$ -Shell Photoabsorption in Lanthanum[†]

J. L. Dehmer*[‡] and A. F. Starace^{§¶}

Departments of Physics and Chemistry, University of Chicago, Chicago, Illinois 60637

(Received 28 June 1971)

An exploratory calculation of the photoabsorption cross section near the $4d$ ionization threshold of lanthanum metal is carried out. The level structure of the configuration $4d^9 4f$ is found to be altered by interaction with the continuum configuration $4d^9 \epsilon f$. The Fano profile of the resonance above threshold is calculated, as are the oscillator strengths of the discrete states below threshold. Our results provide the ground work for more detailed calculations.

I. INTRODUCTION

This paper presents exploratory theoretical calculations of the $4d$ -shell photoabsorption spectrum in lanthanum, primarily to illustrate the general theory for such spectra presented in Paper

I of this series.¹ The experimental data of Zimkina *et al.*² for La exhibit a 44.5-Mb peak about 13 eV above threshold, and three weak lines within a few eV below threshold. These structures have been interpreted in a preliminary report³ as being due to $4d^{10} \rightarrow 4d^9 4f$ dipole transitions. These transitions

are predicted to account for almost all the strength in the observed spectrum because, owing to a potential barrier, there is excellent overlap of the $4d$ and $4f$ orbits, but very poor overlap between the $4d$ and higher f orbits.³ The energy position of the three most intense lines in La have been obtained approximately by Sugar in Paper II of this series⁴ by application of the methods of theoretical spectroscopy to the $4d^9 4f$ configuration. His analysis represents the first step in a complete theoretical treatment; we illustrate here the remaining steps according to the prescription of Paper I. Our emphasis is on the interaction of the levels of $4d^9 4f$ with the continuum channels $4d^9 \epsilon f$. This interaction shifts the energy positions of the $4d^9 4f$ levels and causes autoionization of the large peak above threshold. Our major result is the calculation of the autoionization profile for this large peak. We also calculate absolute oscillator strengths for the weaker experimental peaks. We compare *ab initio* calculated results with those calculated using the scaling procedure of Paper II for the $4d^9 4f$ energy levels. These preliminary calculations give fair agreement with experiment and indicate how future calculations may produce more accurate results.

II. ZERO-ORDER STATES

The definition of the zero-order states follows from the picture, drawn in I, that rare-earth metals consist of ionic cores embedded in and screened by the electrons of the conduction band. For lanthanum, the atomic $5d$ and $6s^2$ electrons form the conduction band resulting in a trivalent core with the electronic configuration of xenon. Dipole transitions of the type $d \rightarrow f$ from the 1S_0 ground state of this core lead to $J=1$ final states which, in intermediate coupling, are linear combinations of the Russell-Saunders terms 1P_1 , 3D_1 , and 3P_1 .

We have neglected the $d \rightarrow p$ transitions. We have calculated that this process contributes ~ 0.5 Mb to the total cross section in the continuum and can be taken into account separately since the interaction matrix elements between the p and f channels and between the p channels and the $4d^9 4f$ levels were calculated to be < 0.01 a. u.

The radial parts of the zero-order states are calculated with sufficient accuracy using the Herman-Skillman (HS) atomic central potential for La.⁵ Indeed, the $4d$ and $4f$ electrons are screened from the metal by the $5s$ and $5p$ subshells and move in a purely atomic field. The Rydberg and continuum radial functions, on the other hand, are calculated accurately using the atomic potential only inside the core (i. e., $r < 2$ a. u.) and at large distances where the net charge is one. This situation suits the purposes of this calculation, however,

since all the matrix elements used later accumulate their value in the region of overlap between the continuum functions and the $4d$ radial function, i. e., inside the core. The outer electrons do influence the continuum radial functions in the core region through a normalization constant.⁶ In this paper, however, we use the atomic normalization to approximate the normalization representing the density of states in the solid.

III. PREDIAGONALIZED STATES

The first step in the prescription of Paper I is to diagonalize the submatrix $\langle 4d^9 4f \alpha' | H | 4d^9 4f \alpha \rangle$, where α indicates one of the terms 1P_1 , 3D_1 , and 3P_1 . The electrostatic and spin-orbit interactions of these terms are obtained from standard references.⁷ We obtained the parameters ζ_{4d} and ζ_{4f} from Sugar⁸; the relevant Slater integrals were calculated using HS wave functions. It is standard procedure in spectroscopy to consider only those interaction matrix elements which affect the relative separation of these terms. Absolute energies are obtained later (after the calculation in Sec. IV) by setting the lowest energy term exactly equal to the lowest experimentally observed peak; this peak has been verified to correspond to 3P in Paper II. We normalized to this lowest peak rather than to the peak above threshold because (as shown in Fig. 2) there is a difference of an eV or more between the resonance energy and the position of the maximum for the peak above threshold.

The above *ab initio* diagonalization leads to term splittings which are much larger than experiment. In Paper II this problem was handled by multiplying the relevant calculated Slater integrals by a scaling factor of $\sim \frac{2}{3}$. We have therefore also diagonalized the $4d^9 4f$ interaction matrix using a scaling factor of $\frac{2}{3}$. Table I lists the energies obtained from both our *ab initio* and scaled calculations. The eigenvectors of this diagonalization are denoted by $^1P'$, $^3D'$, and $^3P'$, and correspond to the states $|4d^9 4f \beta\rangle$ of Paper I. The main feature of the calculated energies is the large separation of the $^1P'$ level from the other two levels. This is caused by the term $2G^1(4d, 4f)$ in the electrostatic energy of the initial 1P level. Here $G^1(4d, 4f)$ is the Slater integral for electron interaction with exchange of one

TABLE I. Comparison of excitation energies (in eV) for the $J=1$ states of the $4d^9 4f$ configuration.

	$^1P'_1$ ^a	$^1P''_1$ ^b	$^3D'_1$	$^3D''_1$	$^3P'_1$	$^3P''_1$
<i>ab initio</i>	130.7	131.4	103.1	102.7	97.2	96.9
Scaled	119.9	115.3	101.5	101.1	97.2	96.9

^aPrimed terms indicate the prediagonalized states β .

^bDouble-primed terms indicate the γ eigenstates at the resonance energies.

unit of angular momentum. When calculated with HS wave functions $G^1(4d, 4f)$ equals 16.3 eV. (Note that any difference between this part of our calculation and the results of Paper II stems from our use of HS wave functions rather than Hartree-Fock wave functions.)

The second step in the prescription of Paper I is to diagonalize the submatrix $\langle 4d^9\lambda', \epsilon'f, \rho' | H | 4d^9\lambda, \epsilon f, \rho \rangle$, where λ designates the values ${}^2D_{3/2}$ and ${}^2D_{5/2}$ and ρ designates the values 1P_1 , 3D_1 , 3P_1 . We ignore the splitting of the $4d^9$ subshell since it amounts to only ~ 2 eV and is not resolved by experiment. Thus we deal with only a single core level, taken to have binding energy 103.8 eV.⁹

We must now diagonalize the electron-core interaction. The matrix elements of $V_{\text{res}}^{\text{ec}}$ are approximated by

$$\langle 4d^9\epsilon'f^1P | V_{\text{res}}^{\text{ec}} | 4d^9\epsilon f^1P \rangle = \frac{11}{7} R^1(4d, \epsilon'f; \epsilon f, 4d), \quad (1)$$

$$\begin{aligned} \langle 4d^9\epsilon'f^3D | V_{\text{res}}^{\text{ec}} | 4d^9\epsilon f^3D \rangle \\ = \langle 4d^9\epsilon'f^3P | V_{\text{res}}^{\text{ec}} | 4d^9\epsilon f^3P \rangle \\ = -\frac{3}{7} R^1(4d, \epsilon'f; \epsilon f, 4d), \quad (2) \end{aligned}$$

where $\frac{11}{7}$ and $-\frac{3}{7}$ are the appropriate angular factors for the R^1 Slater integral. This approximation is justified by the fact that the major interaction is the one between the continuum f electron and the vacancy in the $4d$ shell. Furthermore, a similar calculation for $4d$ photoabsorption in xenon, in which all matrix elements of $V_{\text{res}}^{\text{ec}}$ were calculated for 1P_1 , showed that the contribution of Eq. (1) amounts to $\approx 83\%$ of the total interaction strength over the energy range from threshold to 1 a.u. above.

As calculated with HS wave functions the integral $R^1(4d, \epsilon'f; \epsilon f, 4d)$ is small, being < 0.066 everywhere. Thus, it is not surprising that the calculated reaction matrices $K(\mathcal{E})$ for the terms 1P , 3D , and 3P were found to be approximately equal to the matrix elements of $V_{\text{res}}^{\text{ec}}$. Since $V_{\text{res}}^{\text{ec}} < 0.1$ everywhere, the eigenfunctions of the continuum channel submatrix hardly differ from the HS Slater determinants. For convenience we use the latter for our prediagonalized continuum states.

IV. RESONANCE ENERGIES

The second-order interaction among the discrete β states due to intermediate continuum states is represented by the matrix $F_{\beta\beta'}(E)$ defined in Eq. (20) of Paper I. The 3×3 matrix $F_{\beta\beta'}(E)$ was constructed according to step (iii) of Paper I at 21 energies E (relative to threshold) within the range -0.5 a.u. $\leq E \leq 2.5$ a.u. The integration over intermediate states was truncated at 8 a.u. The eigenvalues $E_\gamma(E)$ of the matrix $E_\beta\delta_{\beta\beta'} + F_{\beta\beta'}(E)$

are shown in Fig. 1. The resonance energies are obtained graphically by superimposing the curves $y = E_\gamma(E)$ and $y = E$. The resonance condition $E_\gamma(E) = E$ for the γ th level [Eq. (23) of I] is satisfied at the intersection of these two curves.

The energies E_γ satisfying the resonance condition are compared with the energies E_β in Table I. Notice that the energy shifts $E({}^3D'') - E({}^3D')$ and $E({}^3P'') - E({}^3P')$ are ~ -0.4 eV and -0.3 eV, respectively. It will be generally true that levels which occur below threshold will experience a negative shift, decreasing in magnitude with increasing distance from the threshold. This can be seen by inspecting the expression for the first-order shift, i. e., $\Delta E = F_{\beta\beta}(E)$, which is negative below threshold.

Levels above threshold may be raised or lowered by this interaction. In this calculation, $E({}^1P'') - E({}^1P')$ is $+0.7$ eV for the *ab initio* case and -4.5 eV for the scaled case.

The transformation matrix which diagonalizes $E_\beta\delta_{\beta\beta'} + F_{\beta\beta'}(E)$ was found to be very nearly diagonal in both calculations, i. e., the diagonal elements were > 0.9999 . This suggests that it may be possible to determine the energy shift $E_\gamma(E) - E_\beta$ by a first-order perturbation treatment, i. e., $E_\gamma(E) - E_\beta \approx F_{\beta\beta}(E)$.

V. OSCILLATOR STRENGTH DISTRIBUTION

In calculating the oscillator strength above the $4d$ threshold we consider only the 1P continuum

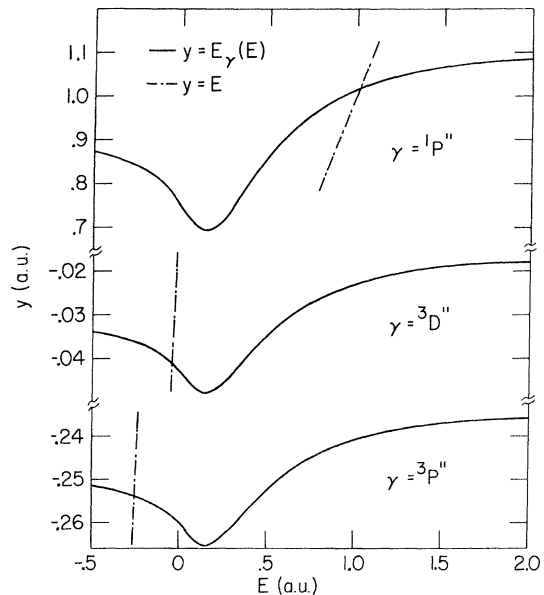


FIG. 1. Energies $E_\gamma(E)$ for the *ab initio* case. The intersection of the two curves $y = E_\gamma(E)$ and $y = E$ represents the position of a resonance energy. The $E_\gamma(E)$ for the scaled case have the same minimum position and similar shape.

channel. This is because the large autoionizing peak above threshold is due to the resonant state $^1P''$, whose overlap with 1P is > 0.997 in both the scaled and the *ab initio* calculations. Hence, this discrete state interacts almost entirely with the 1P continuum. The matrix elements for decay of this state are approximated by Eq. (1) with $\epsilon'f \rightarrow 4f$. The value of $R^1(4d, 4f; \epsilon f, 4d)$ is ~ 0.2 a. u.

Step (iv) of the prescription in Paper I is now quite simple since the reaction matrix $\{\bar{K}(E)\}$ becomes a 1×1 matrix for each energy E . The continuum phase shift due to interaction with the discrete states is now simply $\pi\varphi = \arctan[-\pi\{\bar{K}(E)\}]$. The dipole matrix elements for transition to the augmented discrete states γ_+ in step (v) of Paper I differ from those to the discrete states γ by $\pm 10\%$.

The cross section above threshold is given in Fig. 2 for both the *ab initio* and the scaled calculations. Note that since the $^1P''$ resonance state is approximately isolated, our curves should have the Fano autoionization profile for a q value of ~ 8 .¹⁰ It must be pointed out, however, that Fano's formula assumes that the appropriate matrix elements are constant across the profile. This is distinctly not true for our scaled resonance peak, which occurs in the region of rapid variation of both the augmented discrete states and the energies $E_\gamma(E)$ in Fig. 1.

The reason the scaled calculation produces a

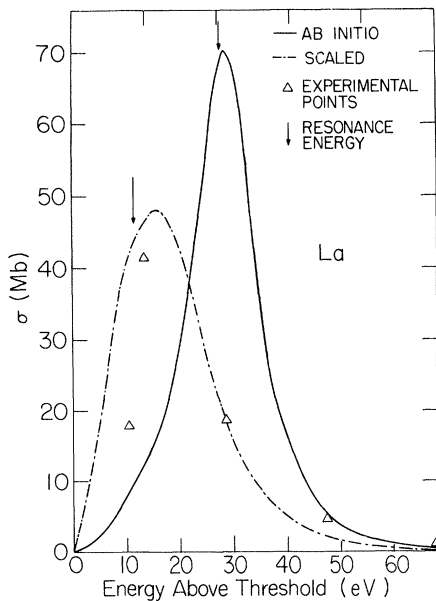


FIG. 2. Photoabsorption cross sections above threshold in the region of the $^1P''$ resonance. Note that the triangle at $E = 13.2$ eV represents the experimentally measured peak maximum (after subtracting background).

TABLE II. Comparison of calculated resonance energies, peak positions, and oscillator strengths for both *ab initio* and scaled calculations.

	Energy positions (eV)			Oscillator strengths	
	<i>ab initio</i>	Scaled	Expt	<i>ab initio</i>	Scaled
$^1P_1''$	131.4	115.3	...	11.65 ^a	9.91 ^a
Peak maximum	132.4	119.6	117		
$^3D_1''$	102.7	101.1	101.6	0.0140	0.0341
$^3P_1''$	96.9	96.9	96.9	0.0021	0.0035

^aThese numbers represent the oscillator strength integrated over the resonance profile.

lower peak height than does the *ab initio* calculation is that the autoionization matrix elements are larger in the vicinity of the scaled peak than in the vicinity of the *ab initio* peak. Hence, the scaled profile is both lower and wider [cf. Eq. (57) of I]. It is also in better agreement with the experimental points, for which background has been subtracted in Fig. 2. Note that the energy of the peak in both calculations is significantly higher than the resonance energies. The integrated oscillator strength for each calculation is given in Table II and is found to be close to 10 electrons. Also in Table II are the resonance energies and the energies of the peak maxima for each calculation.

The oscillator strengths for transition to the $^3D''$ and $^3P''$ levels below threshold were calculated according to Eqs. (44) and (45) of I. These are listed together with the calculated energies for these levels in Table II. Experimentally, the intensity of the $^3D''$ line is ≈ 7 times greater than that of the $^3P''$ line. Our calculated ratios are 7 and 10 for the *ab initio* and scaled calculations, respectively. We do not attach any special significance to the better agreement of the *ab initio* calculation in this case. Since both calculations give about the right ratio we regard this as further confirmation of the level assignments. The very weak observed peak at 103.7 eV might be due to a $4d \rightarrow p$ transition such as are observed in the region of threshold in xenon.¹¹

VI. DISCUSSION

We can draw several conclusions from this exploratory calculation which bear quite generally on future calculations of $4d$ photoabsorption in rare earths and in analogous cases such as $3p$ photoabsorption in the transition metals.

(i) Scaling of appropriate Slater integrals produces energy levels of the $4d^9 4f$ configuration which are in accord with experiment. This scaling substitutes for explicit consideration of the highly excited configurations which interact with the $4d^9 4f$ configuration.¹² These highly excited configurations would alter the discrete-continuum transition matrix elements and it is not clear how to account

for this alteration when using the scaling procedure.

(ii) The scale factors resulting from a spectroscopic treatment serve as approximate input to a calculation based on Paper I since the $4d^9 4f$ energies are shifted by the discrete-continuum interaction. Furthermore, calculated peaks do not lie at the resonance energies in the autoionization region. Therefore, the spectrum can be fit in this way only by an iterative procedure.

(iii) As is evident from points (i) and (ii), a theoretical justification for the scaling factor is a major task for future theoretical work, especially since the theory presented in Paper I produces quantitative agreement with experiment only when the scaling procedure is employed.

(iv) It seems that the continuum electron-ionic core interaction for rare earths is not significant. If necessary, it can be treated by using the first-order approximation for the reaction matrix of

Paper I, i. e., $K(\mathcal{S}) \approx V_{r_{\text{res}}}^{\text{oc}}$. Note that the corresponding intrachannel interaction in xenon has a major influence on the $4d$ -shell photoabsorption spectrum,¹³ but is suddenly reduced in the lanthanides.

(v) The effect of correlations in the ground state of the rare earths is unknown. Since some of these correlations include the Slater integral $G^1(4d, 4f) = 16.3$ eV we anticipate that they will prove important for more detailed calculations of photoabsorption.

(vi) Our calculation indicates that the energy shifts between the β and γ states are given quite accurately by $E_\gamma(E) - E_\beta \approx F_{\beta\beta}(E)$. This may prove an important simplification for calculations of other rare-earth spectra.

ACKNOWLEDGMENT

We wish to thank Professor U. Fano for a critical reading of the manuscript.

[†]Work supported by U. S. Atomic Energy Commission, Contract No. COO-1674-48.

*National Science Foundation Trainee, Department of Chemistry.

[‡]Present address: Argonne National Laboratory, Argonne, Ill. 60439.

[§]National Science Foundation Graduate Fellow.

[¶]Present address: Department of Physics, Imperial College, London, S.W. 7, England.

¹A. F. Starace, first preceding paper, Phys. Rev. B **5**, 1773 (1972), hereafter referred to as Paper I.

²T. M. Zimkina, V. A. Fomichev, S. A. Gribovskii, and I. I. Zhukova, Fiz. Tverd. Tela **9**, 1447 (1967); **9**, 1490 (1967) [Sov. Phys. Solid State **9**, 1128 (1967); **9**, 1163 (1967)]; T. M. Zimkina and S. A. Gribovskii, J. Phys. (Paris) (to be published).

³J. L. Dehmer, A. F. Starace, U. Fano, J. Sugar, and J. W. Cooper, Phys. Rev. Letters **26**, 1521 (1971).

⁴J. Sugar, second preceding paper, Phys. Rev. B **5**, 1785 (1972), hereafter referred to as Paper II.

⁵F. Herman and S. Skillman, *Atomic Structure Cal-*

culations (Prentice-Hall, Englewood Cliffs, N. J., 1963).

⁶J. L. Dehmer and U. Fano, Phys. Rev. A **2**, 304 (1970), Sec. V.

⁷See, e.g., E. U. Condon and G. H. Shortley, *The Theory of Atomic Spectra* (Cambridge U. P., New York, 1935), p. 299; U. Fano and G. Racah, *Irreducible Tensorial Sets* (Academic, New York, 1959), Chap. 16.

⁸J. Sugar (private communication); $\xi_{4d} = 1.2$ eV, $\xi_{4f} = 0.07981$ eV.

⁹W. Lotz, J. Opt. Soc. Am. **60**, 206 (1970). The energy 103.8 eV represents the weighted average of the binding energies of the $^2D_{5/2}$ and $^2D_{3/2}$ levels of the $4d^9$ core, which are split by 2 eV. The absolute error of these binding energies is less than 2 eV.

¹⁰U. Fano, Phys. Rev. **124**, 1866 (1961).

¹¹R. Haensel, G. Keitel, P. Schreiber, and C. Kunz, Phys. Rev. Letters **22**, 398 (1969).

¹²J. C. Morrison and K. Rajnak, Phys. Rev. A **4**, 536 (1971); D. J. Newman and C. D. Taylor, J. Phys. B **4**, 241 (1971).

¹³A. F. Starace, Phys. Rev. A **2**, 118 (1970).